Control of collective human behavior: Social dynamics beyond modeling

Ilias Panagiotopoulos and Jens Starke*
Institute of Mathematics, University of Rostock, 18057 Rostock, Germany

Wolfram Just
School of Mathematical Sciences, Queen Mary University of London, London E1 4NS, United Kingdom

(Received 6 June 2022; accepted 27 October 2022; published 15 December 2022)

The motion of pedestrians is a paradigmatic phenomenon to study collective human behavior. We propose a model-free approach to analyze the movement of pedestrians in experiments and get a quantitative understanding of crowd dynamics. Using concepts from control and analysis of dynamical systems, we set up a scheme which allows us to identify dynamical unstable signatures in pedestrian flows. These signatures are the building blocks for crowd control and soft management of people and thus result in a fundamental understanding of collective human behavior. Our approach is entirely data driven, and we provide a proof of concept using field and laboratory experiments. In addition, this methodology provides, based on experimental observations, quantitative benchmarks to judge the quality of mathematical models for pedestrian motion.

DOI: 10.1103/PhysRevResearch.4.043190

I. INTRODUCTION AND CONTEXT

Modeling and control of collective human behavior constitute one of the central themes of the 21st century, as, for instance, illustrated by crowd control issues at concerts or sporting events or evacuation procedures for buildings. Most vividly, these aspects are emphasized by extreme events such as the Hillsborough disaster [1], the Duisburg Love Parade disaster [2], or the King's Cross Station fire [3]. Studying and understanding pedestrian dynamics in a qualitative way may have a huge impact on crowd safety (see, e.g., Refs. [4–6]), individual comfort [7], infrastructure design [8], and implementing social distancing to prevent the spreading of diseases such as COVID-19 [9–11].

There exist a large number of simulation programs [12–16] both based on computational fluid dynamics and based on discrete particle simulations impacting on governmental regulations and fire safety codes in many countries [17,18]. In all these contexts, theoretical modeling is in fact quite advanced and often in good agreement with actual data providing suitable input for a number of different standards for the design of critical infrastructure [19,20]. However, these simulation programs miss systematic experimental verification despite the work of a few experts (e.g., Refs. [21–27]), since setting up experiments in a sociotechnological context is a challenge.

Actual experiments in social systems pose a couple of substantial challenges. If we briefly adopt the notation predominantly used in statistics, social sciences, or medical clinical trials, experiments can be broadly grouped in three different categories, namely, statistical surveys where accurate average information about the behavior of individuals can be obtained, observational studies which give detailed information about the dynamics of groups of people, and experimental studies where one impacts on a group of individuals and monitors the dynamical response. Such a classification is not sharp, the borders between the different categories are certainly blurred, and the classification may not fit perfectly in the physics context. Nevertheless, it helps to group the available experimental studies and to clarify our aim. For instance, Refs. [28,29] provide nice and very detailed overviews of properties of pedestrian motion obtained at an aggregate level. Experiments where one records the behavior of groups of pedestrians subjected to static constraints and where one draws fundamental conclusions about the pedestrian flow are described, for instance, in Refs. [30–32], which give, among other things, detailed insight into the structure of the fundamental diagram; in Refs. [33–35], which provide a comparison of actual experiments with models and discuss the identification of parameter choices; in Ref. [26], which nicely illustrates state-of-the-art technology to extract single-trajectory information from experimental observations; and in Ref. [36], which discusses in detail experimental observations to uncover the impact of diversity on the behavior of crowds. Our approach follows the third paradigm, where we aim to investigate the impact of small time-dependent external inputs on the dynamics of a crowd. Thus we broadly follow the concepts of response theory or spectroscopy developed, e.g., in the context of condensed matter physics (see also Ref. [23]). In more detail, we apply, in an experimental setup, control techniques to study and track instabilities and bifurcations, a concept which is a powerful tool for the numerical investigation of nonlinear model equations. A direct analysis of

*jens.starke@uni-rostock.de

pedestrian experiments which uncovers changes in the qualitative dynamical behavior, i.e., an experimental bifurcation analysis, is lacking so far.

For our pedestrian experiments a sufficiently large number of individuals is crucial. Initial experimental trials with periodic boundary conditions where pedestrians entered a corridor repeatedly failed due to individuals memorizing their previous actions, adjusting their behavior, and substantially changing the dynamics of the crowd. As a result, humans in our control experiments were allowed to participate in the experiment only once. Mass events such as football matches or concerts provide many pedestrians when arriving at the location. However, accompanying habits such as predrinking alcohol create difficult nonreproducible circumstances for experiments. Several trials failed as people deliberately disturbed the measurement processes. Reasonable conditions without hiring a large crowd can be found, for example, at public transport hubs during rush hour. We were unable to obtain permission to conduct experiments at bigger stations in Germany (Berlin and Hamburg) or in the UK (London); see, e.g., Ref. [37] for the challenges one faces when one performs large-scale pedestrian experiments in the public transport sector. We finally chose to perform experiments at the Ulmencampus of the University of Rostock, with first-semester students just starting their studies, and field experiments at the pier at Warnemünde port, where passengers are disembarking cruise ships.

As for the actual investigation, we analyze the route choice of individuals belonging to a crowd of people with the same target. This, for instance, could be a situation where people need to quickly move from one train platform to another or where people have to choose a route to the exit of a building. To model such situations in a well-defined setup, we design experiments where individuals aim to reach an exit at the end of a corridor (see Fig. 1). A few meters in front of the exit a triangular obstacle blocks the pedestrians' direct way to the exit and gives them the option to maneuver around the right or left side of it. The pedestrian flux difference between passing left or right of the obstacle is the key quantity to be studied, since this basic quantity gives us information about the route choice of the pedestrians and the crowding in the corridor. Of particular interest will be the effect of the obstacle's position on the flux difference.

The noteworthiness of the current study comes in three parts. Firstly, by varying the position of the obstacle, we succeeded in observing bistable states of the flow of human crowds. As a consequence, our findings indicate that in addition to stable flow patterns observed in experiments there are also unobservable, which means unstable, states which are crucial for understanding the overall global dynamics. Secondly, we successfully applied an adaptive feedback controller to stabilize and reveal such unstable states. Finally, we demonstrate how the features of pedestrian flows can be exploited to implement soft management strategies [38], to achieve crowd control and to minimize crowding. By this, we mean measures which are indicative and provide guidance, such as signage [39].

The impact of our approach is twofold. On the one hand, we are able to propose suitable management and design strategies which minimize crowding and optimize social distancing.

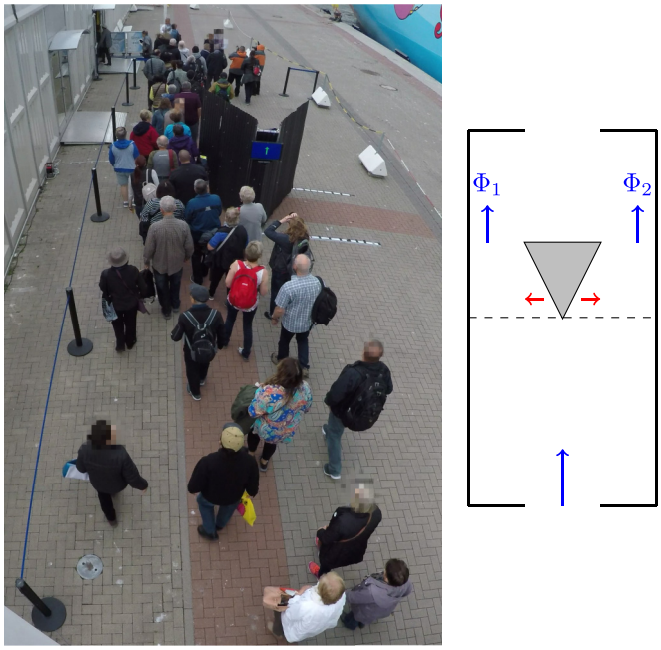

FIG. 1. Left: Route choice experiment of a pedestrian flow passing an obstacle. Right: Schematic setup of the experiment with corridor, obstacle, and pedestrian flows indicated. The crucial parameter is the position of the obstacle, and the relevant observable is given by the flux difference $\varphi = \Phi_1 - \Phi_2$ of pedestrians passing on the left and on the right of the obstacle.

On the other hand, our approach can be used as an analytic tool to gain a better understanding of the dynamics of pedestrians. While our setup is quite basic, it turns out that the experiment we propose shares many features with real-life pedestrian flows. We think our demonstration of successful soft management control strategies has considerable implications for real-life human behavior.

II. HYSTERESIS IN PEDESTRIAN FLOWS

We performed our study at two events with different focus. In the first set of experiments we aimed at a well-defined and reproducible setup using a crowd with lower density, with fewer interpersonal relationships between pedestrians, and with a well-defined pedestrian inflow. Hence we were emulating situations which are found in laboratory experiments in physics or chemistry with a well-defined and reproducible environment. This series of experiments was conducted with first-year students at the beginning of the autumn term at the University of Rostock. The key dynamical findings in this setup, i.e., bistability and hysteresis of the pedestrian flow, were then tested in a real-world setup to ensure that our findings were not triggered by artifacts of laboratory setups. The second type of study was performed on a pier in the Warnemünde port where a crowd of people had just disembarked from a cruise ship.

In both experiments, people had to enter and exit a rectangular corridor designated by queue barriers. There was a single entrance and a single exit, which all participants were aiming for; see Fig. 1. A triangular obstacle was placed in the pedestrians' way to this single exit. The pedestrians passing

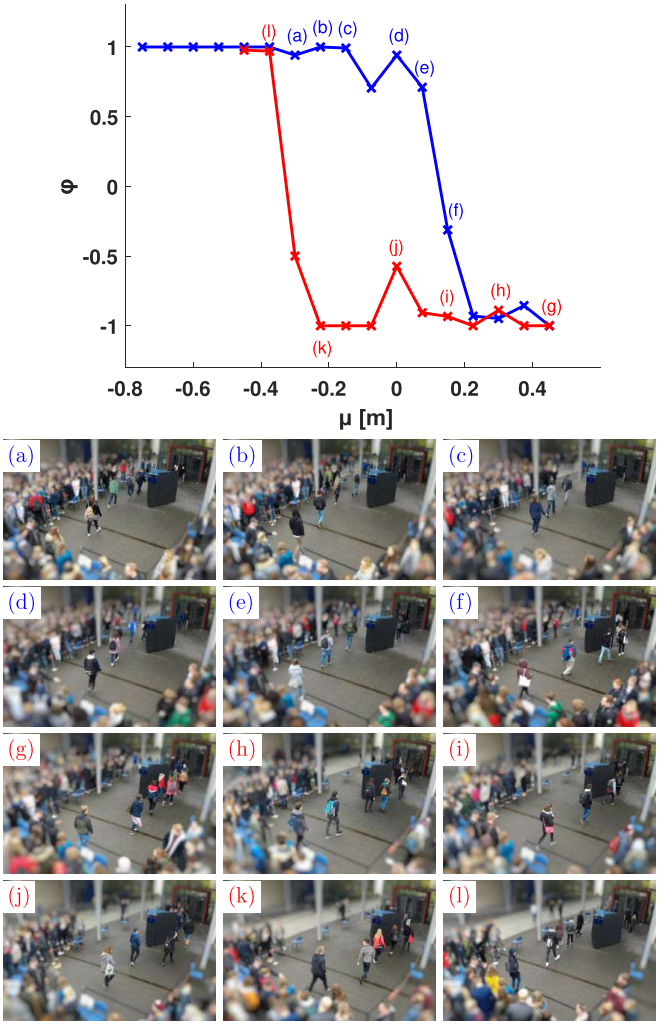

FIG. 2. Route choice experiment at Ulmencampus, University of Rostock. Top: measured mean flux difference as a function of the obstacle position, for upsweep (blue) and downsweep (red) of the system parameter, showing hysteresis. Bottom [(a)–(l)]: snapshots of the actual pedestrian configurations for different values of the obstacle position (see labels).

the obstacle on either side were counted, where, in this paper, the left and right sides are described from the pedestrians' point of view. The obstacle had the shape of an isosceles triangle, with two sides being 2.2 m long and the third one being 1.8 m long. The height of the obstacle was 2.4 m.

In the experiment conducted at Ulmencampus (see Fig. 2 and the blurred video in the Supplemental Material [40]), our designated corridor was placed in front of the entrance of a lecture theater. The dimensions of the corridor were 14 m long and 6 m wide. The width of the entrance and the exit was 1.2 m. There was an obstacle in the pedestrians' way, 6 m after the entrance (see Fig. 1). Students wanted to enter the lecture theater and were asked to wait briefly at the entrance of the corridor, so that a constant inflow rate of about 0.6 persons/s could be realized. In total, about 600 students participated. In the Warnemünde port experiment the corridor was 16 m long and 6 m wide, while the width of the entrance and the exit was 5 m. The obstacle was placed 8 m after the entrance. Over 1000 pedestrians participated, with an average inflow rate of around 1.5 persons/s. Participants were people of different ages and with no knowledge of the infrastructure but with the desire to reach their target destination quickly. During the experiments, we systematically moved the obstacle to different positions and recorded the corresponding value of the flux difference φ_t. The process of moving the obstacle slowly was barely noticeable by the pedestrians, meaning that in both cases, we performed a quasistationary parameter change, i.e., after each small increment we allowed the system to relax to a stationary state before we measured the current.

The variable of interest is a time-dependent flux difference φ_t, which means the choice people make of passing to the left or right of the obstacle. To measure this, we define φ_t to be the mean of the last eight pedestrians' choices, with $+1$ for each one choosing the left side and -1 for the right side. We use the convention of assigning positive values to people choosing the left side of the obstacle, $p_t = 1$, and negative values to the other side, $p_t = -1$, where t labels the time. Since the counter p_t is a strongly fluctuating quantity, in particular in cases with low-density pedestrian flows, we take an average of the last eight pedestrians' crossings, $\varphi_t = 1/8 \cdot (p_t + p_{t-1} + \cdots + p_{t-7})$, to measure the route choice difference. The window size of 8 results in a discrete measure φ_t which can take nine different values with resolution ± 0.25. This quantity provides enough information for our data-based and model-free approach. Most importantly, no advanced tools for measuring the speed or the distances between pedestrians were needed.

The results from the experiment at the Ulmencampus are presented in Fig. 2. With $\mu = 0$ denoting the center of the corridor, the obstacle was moved from negative to positive positions by small increments of 0.075 m and then back toward its initial positions. For each obstacle position, we allowed the flow to attain a new stationary state before we moved the obstacle again. During this procedure, we observed a sudden change in people's choice for two different positions of the obstacle. This phenomenon is reflected by the mean flux difference jumping from positive to negative values at around $\mu = 0.15$ m and then from negative to positive at about $\mu = -0.225$ m; see Fig. 2. The bottom part of Fig. 2 shows the pedestrians' walking choices throughout the obstacle sweep. From the obstacle sweep, we observed that for any position $\mu \in [-0.225\text{ m}, 0.15\text{ m}]$ there are two different states of the system which seem to be stable. When the obstacle position is changed, the choice of the pedestrians depends on the previous state, which leads to a hysteresis phenomenon.

The results of the second series of experiments are shown in Fig. 3. In these experiments, passengers wanted to leave the pier at Warnemünde port. We had a quite diverse crowd at our disposal with individuals of a large range of ages and different nationalities, where pedestrians had no knowledge of the infrastructure they were about to cross. Passengers wanted not only to leave the pier as quickly as possible but also to stay close to their friends and families. Unlike the first type of experiments, the second setup contained elements which broke the left-right symmetry. The dependence of the flux difference on the obstacle position is summarized in the top panel of Fig. 3.

From the obstacle sweep, for any position $\mu \in [0.3\text{ m}, 0.75\text{ m}]$ there are two different states of the system

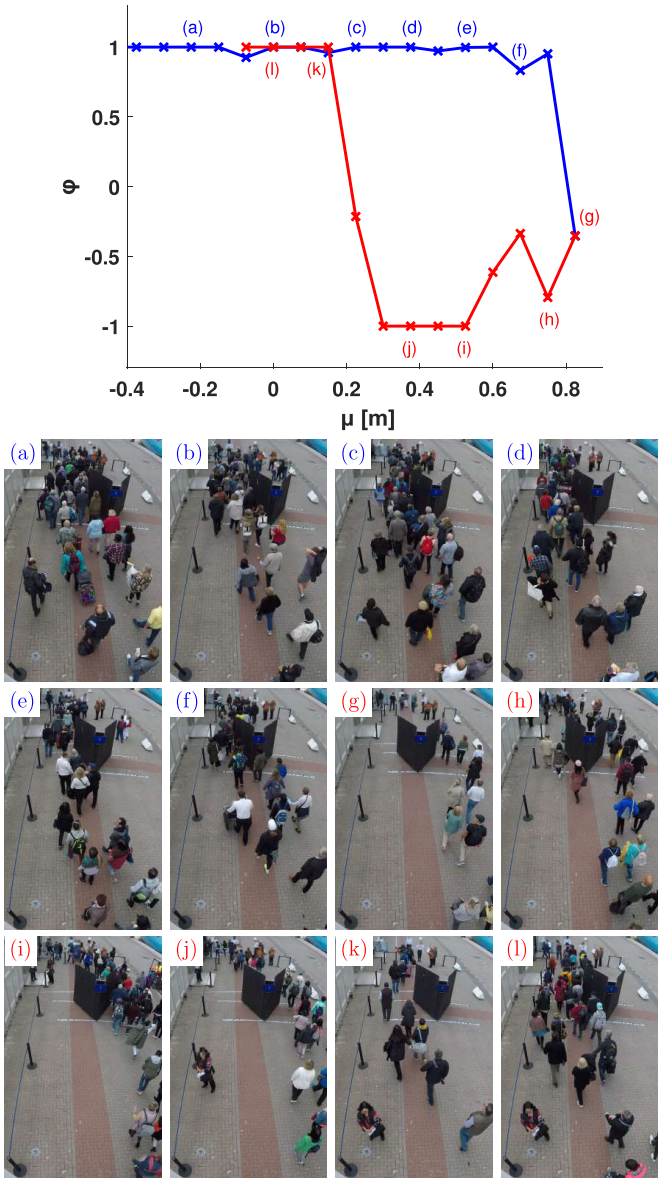

FIG. 3. Route choice experiment at the Warnemünde port. Top: measured mean flux difference as a function of the obstacle position, for upsweep (blue) and downsweep (red), showing hysteresis. Bottom [(a)–(l)]: snapshots of the actual pedestrian configurations for different values of the obstacle position (see labels).

which seem to be stable. The hysteresis is, however, not symmetric, as the interval of offsets μ for which we observe bistability is not centered around $\mu = 0$. There is a clear bias towards one side. Indeed, that was expected since the Cruise Center was to the left and parallel to our designated corridor. Hence pedestrians favored passing on the left side of the obstacle. Nevertheless, we still observed the previously recorded hysteresis phenomenon. In particular, our findings are robust under real-world conditions, where, e.g., we do not monitor the inflow of pedestrians. Furthermore, hysteresis still persists under other inhomogeneities which occur frequently in social groups. For instance, we observed small groups of passengers, such as families or friends, walking together or slowing down to wait for each other. We also observed moments where the density of pedestrians was higher or lower or even moments when there was a small gap in the flow. Neither of these imperfections had an impact on the occurrence of the hysteresis phenomenon, which can hence be considered as a fairly robust property of a pedestrian flow. Additionally, the phenomenon observed does not seem to be a cultural characteristic since the participants in the second series of experiments were tourists of different nationalities.

The results from both series of experiments indicate that for a range of positions of the obstacle, two different states of the system coexist. The bistability observed in this system does not require a special type of geometric symmetry. It is robust against a bias, as illustrated in the results from the experiment at Warnemünde port. The hysteresis phenomenon also appears in a setup where the discrete nature of the measured flux difference is noticeable. We conclude that the dynamical signature, the hysteresis caused by the route choice, is a stable phenomenon which does not just occur under laboratory conditions, but reflects real-life situations of pedestrian flows.

III. NONINVASIVE CONTROL: SOFT MANAGEMENT STRATEGIES

Crowd or traffic management [41–43] can be considered as a particularly challenging engineering control problem where one uses small control inputs for guiding people. Such soft strategies are actions, suggestions, or guidelines that pedestrians could ignore such as markings on the floor, signs, or traffic indicators for different routes. Control with minimal invasion has been reemphasized in science, in particular in the context of controlling complex dynamical behavior [44]. Feedback control exploits the dynamical features of the underlying dynamics, making a large variety of potential target states accessible. In addition, control can also be used to explore the features of a system (see, e.g., Refs. [45–50]), where one mimics within an experimental setup continuation techniques used for bifurcation analysis. Hence control in this context has a second facet, namely, employing the technique for the analysis and spectroscopy of complex dynamical behavior. Within our experimental setup we have the ideal test bed to study noninvasive control in a sociodynamical context. The measurements presented in the previous section and the general theory of dynamical systems suggest that an additional, unstable and therefore unobservable state of the system exists in the bistability region. As we operate in the neighborhood of a stationary state, control is possible with minimal control forces. We aim to control an unknown unstable steady state with asymptotically vanishing control force, while at the same time we have limited possibilities to act on our system. We employ here soft management strategies, i.e., using signs or traffic lights, as opposed to hard management strategies which are invasive such as barriers or bouncers.

Controlling unknown states is quite well known in engineering and can be achieved by a state observer. As for the actual control algorithm we follow a suggestion of Ref. [51] which in fact is a simple realization of feedback control with a state observer. To illustrate the basic idea, recall that the flux difference measuring the pedestrians choice, φ_t, is the quantity of interest. Assume for the purpose of illustration that the

time evolution can be approximately captured by an unknown differential equation of the type $\dot{\varphi}_t = G(\varphi_t)$ with unstable stationary state φ_*, which implies $G(\varphi_*) = 0$. Adding a control force results in $\dot{\varphi}_t = \tilde{G}(\varphi_t, a(y_t - \varphi_t)) = G(\varphi_t) + a(y_t - \varphi_t)$ with a being the gain of the control loop. We here consider the simple case that the dynamics of the control device is governed by a linear law $\dot{y}_t = b(y_t - \varphi_t)$ with filter parameter b. The dynamical state y_t of the controller estimates the value of this unknown unstable state and can be considered as the simplest incarnation of a so-called state observer. The control signal $y_t - \varphi_t$ is then fed back to our original dynamical system resulting in the closed-loop dynamics $\dot{\varphi}_t = \tilde{G}(\varphi_t, a(y_t - \varphi_t))$ with a being the gain of the control loop. The fixed point of this closed-loop dynamics is clearly given by $y_* = \varphi_*$ and $G(\varphi_*) = 0$, i.e., y_* estimates the unknown fixed point which coincides with a fixed point φ_* of the original equation of motion. Furthermore, the feasibility of the control algorithm can be established by a simple linear stability analysis. If φ_* is an unstable fixed point with positive eigenvalue $G'(\varphi_*) > 0$, then linear stability analysis easily shows that stability of the closed-loop dynamics with the state observer is achieved if $b > 0$ and $a > G'(\varphi_*) + b$. In particular, the actual control signal becomes small and asymptotically tends to zero, so that the approach works with tiny control forces. Implementation does not require any knowledge about the stationary state or the underlying equations of motion. This, in practice, means that the external force induced by signs is in principle able to drive the system to unobservable states, and it vanishes when the system operates around an unstable fixed point.

The diagram in Fig. 2 is the result of a fairly complex dynamical system with many degrees of freedom, but it resembles a structure which can also be seen in a low-dimensional effective equation of motion. Equation-free analysis [52] aims at reducing the dynamics of a complex system, normally given in terms of a high-dimensional system of differential equations, to a low-dimensional effective equation of motion just based on numerical simulations. Here we take this idea a crucial step further [47,48]. We explore whether it is possible to use measurements and control techniques in our pedestrian flow to identify signatures of such a low-dimensional effective equation of motion. Using the analogy with bifurcation analysis, the result shown in Fig. 2 suggests that there exists an additional unstable branch of states. Such unstable flow patterns correspond to an unstable fixed point in an effective low-dimensional description. Using the control algorithm described above, we aim to track unstable, i.e., unobservable, states, in relation to the obstacle position μ. Unlike in numerical simulations, where initial conditions are at the disposal of the programmer, we have only very limited control, if any, over the initial state of the system. In practice we just let pedestrians enter the corridor. We are, however, able to change the position of the obstacle, μ, and we can set the initial state of the observer variable, $y_{t=0}$, which estimates the unknown effective fixed point and then dynamically adjusts to the true value of the originally unstable flux difference.

The experiments with control were conducted at the Ulmencampus with the same configuration as described in the previous section. To implement a soft management strategy, we displayed an arrow on a monitor mounted on the obstacle, but we did not give any further incentive to the pedestrians to follow this sign. For the control scheme the arrow was inclined and magnified giving the pedestrians an indication regarding on which side to pass the obstacle. The inclination and size of the arrow were adjusted proportionally to the control signal $y_t - \varphi_t$, with positive or negative values corresponding to an arrow inclined towards the right or left, respectively. Successful control is indicated by the system fluctuating around a state or, equivalently, reaching a new steady state, with small control signal $y_t - \varphi_t$.

As for the protocol of the experiment with control, the following steps were performed. First, we made a prediction for an unstable state. The choice of these initial values was made based on the sweep diagram as depicted in Fig. 2. Although the diagram is not perfectly symmetric, it appears that the tipping points are around $(\mu, \varphi) = (-0.3, -1)$ and $(\mu, \varphi) = (0.3, 1)$. As a result, we expected the unknown steady states to lie in the vicinity of the line connecting these two points. Based on the sweep diagram of Fig. 2 we initialized our experiment with $\mu = 0$. For the differential equation governing the state observer $\dot{y}_t = b(y_t - \varphi_t)$ we chose $y_{t=0} = 0$ and $b = 0.05$. The parameter a that scales the arrow accordingly was chosen to be $a = 6$. In contrast to a numerical experiment where a model for the system under investigation is available, the pedestrians' state could not be set at will. As a result, we had no way to initialize the pedestrians at a given state. Instead, pedestrians started entering the corridor, walking towards the end of it, and being influenced by the arrows displayed at the front of the obstacle. As explained above, reaching a new steady state is equivalent to the system fluctuating around a state with small control signal $y_t - \varphi_t$. When this happened, we recorded the value around which φ_t fluctuates as a new steady state. At this point, we were ready to move to the next parameter value. Pedestrians kept walking inside the corridor as we moved the obstacle to $\mu = 0.075$ m and initialized the differential equation governing the state observer with $y_{t=0} = 0.25$. As soon as the experiment for this position of the obstacle was successful, we continued with two more cases: the case of $\mu = 0.15$ m, $y_{t=0} = 0.5$ and the case of $\mu = 0.225$ m, $y_{t=0} = 0.75$.

The results of the experiment with control are summarized in Fig. 4. Students were asked to walk through the corridor only once, as people's memories of going through the corridor several times would potentially alter the results. We conducted the experiment for four different positions of the obstacle, and we managed to reveal additional unstable states; see the green circles in the top panel of Fig. 4. The middle part of Fig. 4 shows time traces of the various relevant quantities. The state of the controller y_t (red) quickly approaches the flux difference of the unstable state and thus estimates the unobservable state successfully. The flux difference φ_t (blue) approaches the same value but shows larger fluctuations. These fluctuations are caused by the intrinsic discrete nature of the measured flow φ_t, which comes in units of 0.25. Convergence is better visible when we smooth the data by a Cesàro average defined as $c_t = \sum_{k=1}^{t} p_k/t$ (cyan). Finally we show as well the pedestrians' choices $p_t = \pm 1$ (magenta circles), which clearly demonstrate that the pedestrian flow under control is channeled along both sides of the obstacle. Above all, the control signal $y_t - \varphi_t$ becomes small when successful control is achieved so that the

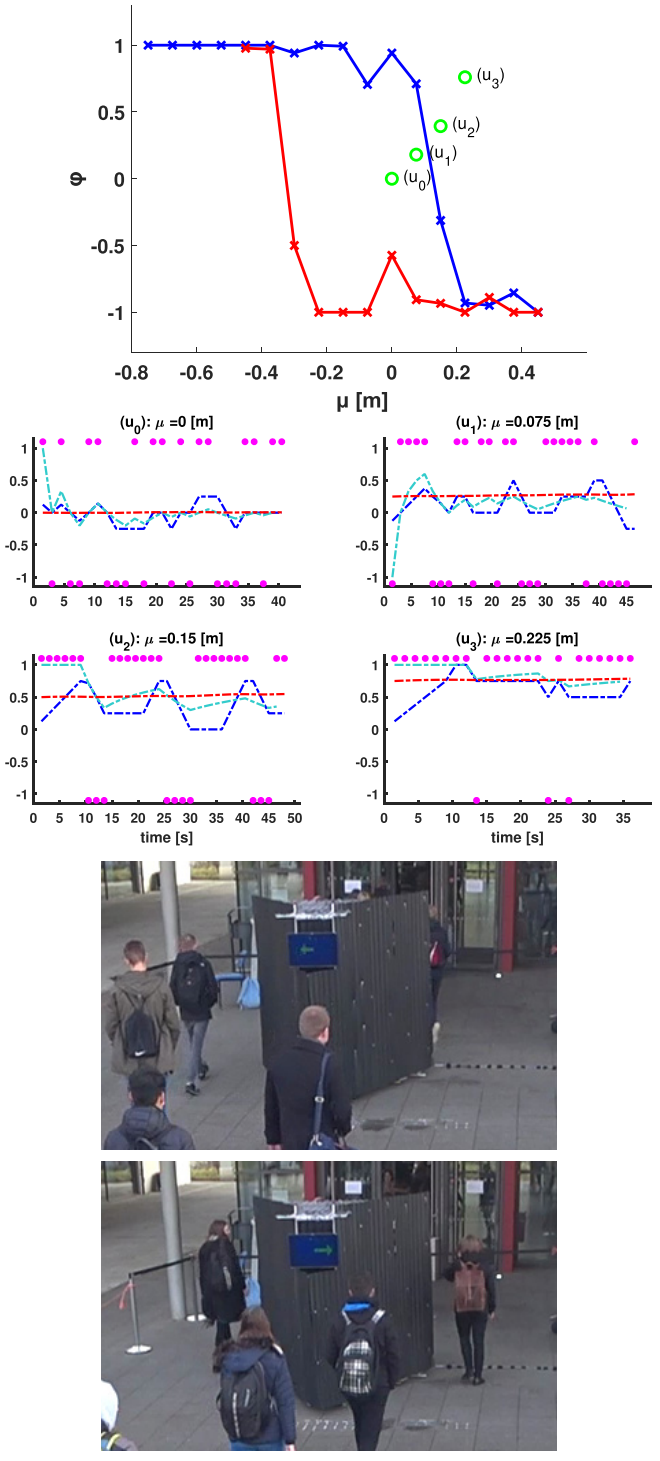

FIG. 4. Control of pedestrian flows at the Ulmencampus. Top: flux difference as a function of the obstacle position. Stabilized unstable states (green circles) for different positions of the obstacle; for comparison, the flux difference without control (see Fig. 2) is shown for the upsweep (blue) and the downsweep (red) of the parameter. Middle: the measured control flux difference φ_t as a function of time t (blue, actual flux difference; cyan, Cesàro average,; see text for details), the state of the controller y_t which estimates the target state (red), and the time trace of the pedestrian count passing by the obstacle, i.e., p_t (magenta circles). Bottom: snapshots of actual pedestrian configurations during control for $\mu = 0$. Control is implemented by the green arrow displayed on the screen.

states shown in Fig. 4 are unstable solutions of an underlying dynamical system.

In addition to the data obtained from this experiment, the top panel of Fig. 4 also contains the mean flux difference observed in the experiment without control (cf. Fig. 2). Some of the controlled states are almost outside the observed hysteresis region. The actual bistability region is certainly larger than recorded since noise, imperfections, and finite-size effects render some of the observable stable states unstable, a phenomenon which is prevalent at the boundaries of the bistability region.

Unlike the uncontrolled pedestrian flow, the flow subjected to the control shows less crowding. A close inspection of the controlled states reveals that the actual pedestrian flow is split into two parts with pedestrians passing by the obstacle on the left side and on the right side (see, e.g., magenta circles in the middle part of Fig. 4 and the photos in the bottom part). Effectively, the pedestrian flow becomes less crowded, and social distancing between pedestrians is enhanced. We achieved this by a minimally invasive control force which eventually becomes small. In addition, the optimal obstacle position for splitting the flow in the current symmetric setup is certainly the position without offset, $\mu = 0$, as the controlled flow difference becomes minimal in this setup. While this feature is a consequence of the symmetries shared by our setup, the optimal obstacle position is less obvious in asymmetric situations (cf. Fig. 3).

In summary, we have implemented a soft management strategy where the control input becomes small when the target state is reached. We have achieved that success by exploiting the system dynamics. Our showcase proves that soft management strategies can give a better level of service if suitable unstable states in pedestrian flows can be identified, leading finally to more efficient crowd management.

IV. MICROSCOPIC MODELS VERSUS THE MODEL-FREE APPROACH

The phenomena observed and described through the conducted experiments provide a good test for the various models of crowd behavior; see, e.g., Refs. [5,53–55] for a review. One popular model which has been extensively used for pedestrian simulations is the *social force model* [56]. According to this model, pedestrians are described as particles, and their motion is the result of social forces acting on them. These forces reflect the impact of their psychology and surroundings. The motion for pedestrian i is given by its acceleration

$$\ddot{\mathbf{x}}_i = \mathbf{F}_i + \sum_j \mathbf{f}_{ij} + \mathbf{f}_i^B, \tag{1}$$

where $\mathbf{F}_i$ is the target force that drives an individual towards a specific target with a desired velocity, $\mathbf{f}_{ij}$ are the interaction forces between pedestrians i and j, and $\mathbf{f}_i^B$ is the external repulsive force taking the effect of the walls and the obstacles into account. The target force is given by

$$\mathbf{F}_i = \frac{1}{\tau}(v_i \mathbf{e}_i - \dot{\mathbf{x}}), \tag{2}$$

where τ denotes the reaction time, v_i is the desired speed of pedestrian i, and $\mathbf{e}_i$ is their normalized target direction. The

latter was adjusted to include the tendency to follow people around (see Ref. [57]). Specifically, the target direction of each pedestrian is a linear combination of the direction to the exit, $\mathbf{e}_\parallel$, and a weighted mean of the velocities $\langle \dot{\mathbf{x}}_j \rangle_i$ over pedestrians j in the neighborhood of pedestrian i

$$\mathbf{e}_i = \frac{(1-\lambda)\mathbf{e}_\parallel + \lambda \langle \dot{\mathbf{x}}_j \rangle_i}{\|(1-\lambda)\mathbf{e}_\parallel + \lambda \langle \dot{\mathbf{x}}_j \rangle_i\|}, \tag{3}$$

where λ denotes the *lemming parameter* which measures the psychological impact by pedestrians in the neighborhood. See Refs. [57,58] for details.

Control by signage, traffic lights, or arrows is an inherently complex process involving perception and psychology. Here we just map this complex process to an adjustment of the target direction. To implement the soft control strategy of our experiment (see Fig. 4), i.e., to feed the control input to the model, we update the target direction $\mathbf{e}_i$ of pedestrian i. This results in a target direction with control

$$\mathbf{e}_i^c = \frac{\mathbf{e}_i + a(y-\varphi)\mathbf{n}_\perp}{\|\mathbf{e}_i + a(y-\varphi)\mathbf{n}_\perp\|}, \tag{4}$$

where $\mathbf{n}_\perp$ denotes a vector perpendicular to the walls of the corridor. To take the local character of our experimental setup into account, which just relies on displaying arrows on the monitor in front of the obstacle, we update the control term $\mathbf{e}_i^c$ only for pedestrians inside a small rectangular area in front of the obstacle visualized as a red box in the bottom part of Fig. 5. In order to verify this model we have performed a series of particle simulations similar to the experiments. The entire geometric configuration, e.g., corridor, obstacle, and entrance, was the same as in the experiment at Ulmencampus. We also ensured that there were always eight pedestrians inside the corridor.

For the numerical integration of the model, we take a lemming parameter $\lambda = 0.45$, a pedestrian-obstacle length scale of 1.5 m, a pedestrian-pedestrian repulsion parameter of 10 m/s^2 and a pedestrian-pedestrian interaction range of 2 m. The control area was a rectangular area of width 0.7 m and length 1.5 m placed (its closer side) 1.3 m in front of the obstacle. The control area was shifted together with the obstacle so that its center was always the tip of the triangular obstacle. The rest of the parameters of the simulation can be found in Refs. [57,58].

While a microscopic numerical simulation allows for the application of the most subtle control algorithm, we deliberately stayed with the protocol used in our experimental setup. We first emulated a parameter up- and downsweep to record the flux difference without control. In the second part of the numerical simulations we applied the control scheme described above. Figure 5 summarizes our findings. In the top panel the blue and red lines correspond to the mean value of the measure φ without control for different positions of the obstacle. Clearly, the experimental hysteresis phenomenon is reproduced even at a quantitative level (see Fig. 2). The green symbols show the states subjected to control. Again a remarkable quantitative agreement between the simulation results (circles) and experimental data (crosses) is found. The middle part of the figure shows the time series of the measure φ (blue line) and the controller variable y (red line) for four states of the system. The magenta circles indicate the

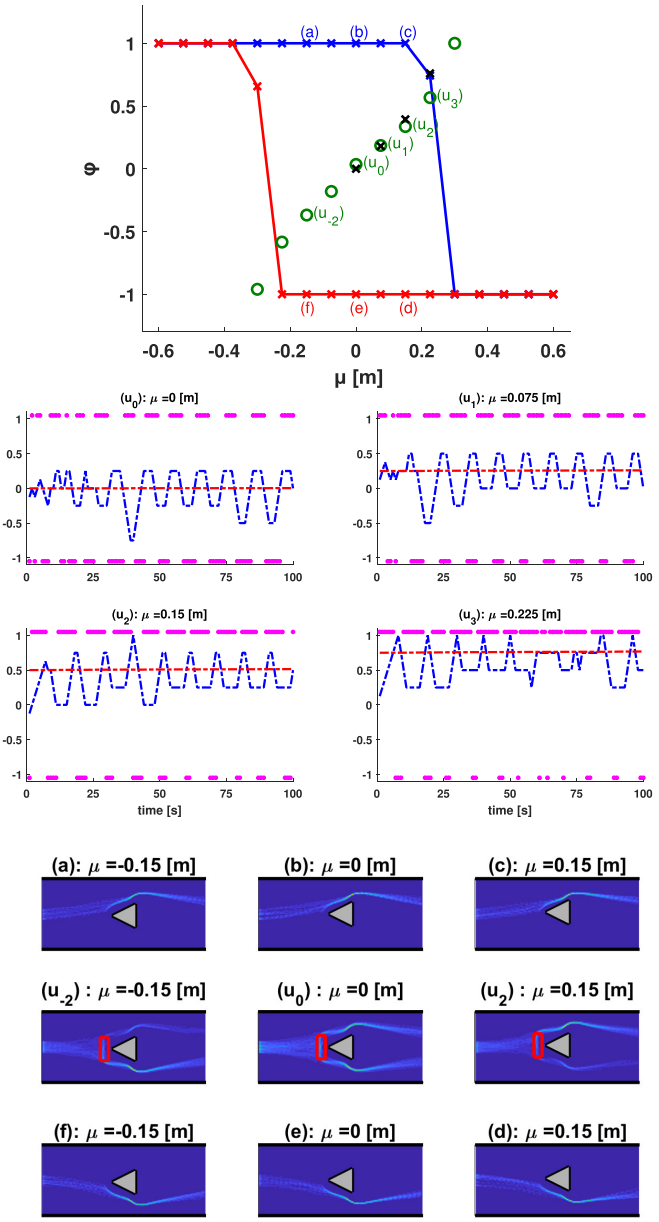

FIG. 5. Numerical simulations of control of pedestrian flows. Top: the flux difference φ is plotted over the obstacle position. Stabilized target states (green circles) for different positions of the obstacle reveal the unstable branch. For comparison, experimental results are shown by black crosses (see Fig. 4). The flux difference without control is shown for the upsweep (blue) and downsweep (red) of the parameter (compare with Fig. 2). Middle: the measured control flux difference φ_t as a function of time (blue, actual flux difference), the state of the controller y_t which estimates the target state (red), and the time trace of the pedestrian count passing by the obstacle, p_t (magenta circles). Bottom: density plots of pedestrians for different positions of the obstacle (gray triangle) without control—parameter upsweep [(a)–(c)] and parameter downsweep [(d)–(f)]—and density plots with control (u_{-2}, u_0, and u_2). The red rectangle in front of the obstacle indicates the control area; only pedestrians in this area are affected by the control input.

choice of each pedestrian. Even these microscopic features of the simulations coincide remarkably well with the actual

experimental time traces of Fig. 4. Similar to the results from the experiment, we can see some fluctuation around a steady state. The bottom part of the figure consists of density plots of trajectories of pedestrians during the control-free simulations for the parameter upsweep [Figs. 5(a)–5(c)] and downsweep [Figs. 5(d)–5(f)] and density plots during the control procedure (u_{-2}, u_0, and u_2). Comparing the density plots subjected to control (panels corresponding to u_{-2}, u_0, and u_2) with those without control [Figs. 5(a)–5(f)], we clearly see that the control strategy manages to disentangle the pedestrian flow efficiently. Furthermore, if we switch off the control, the system returns to the stable branches, thus giving again evidence that the stabilized patterns are unstable states of the system.

We thus have compelling evidence that the model outlined in this section is able to capture details of the experimental pedestrian flow even at a quantitative level. It is, however, important to stress that such an accurate model is by no means needed to analyze pedestrian flows within our model-free approach. The detection of suitable unstable states which can be used for a soft management strategy can be accomplished solely by a simple control tool. The outcome of the procedure is a bifurcation analysis at a macroscopic level which is sufficient to uncover the relevant dynamical features of our flow experiment. Nevertheless, accurate microscopic models have their virtue as they allow for prediction and for the implementation of sophisticated management strategies. The accuracy of such models can then still be benchmarked by a model-free analysis.

V. DISCUSSION

We have proposed an experimental test bed which is appropriate for implementing and testing soft management strategies for pedestrian flows. In particular, we succeeded in extracting the dynamic features of the walking behavior of pedestrians without the need for a mathematical model. Above all, bifurcation scenarios were detected which can be exploited to manage crowds in a real-world scenario. Since the outlined approach does not rely on any model, the findings are robust and stable with regard to imperfections and noise. In addition, the protocol employed here allows one to validate mathematical models of social behavior in a quantitative way. In particular, our method confirms the validity of social force and related models as long as crucial ingredients such as the lemming effect are properly accounted for. The latter provides an efficient way to take into account the psychology of individuals and its impact on the overall pedestrian flow. Under such conditions we obtain a quite remarkable quantitative agreement between experiment and model, which *a posteriori* confirms the advanced stage of modeling of social behavior.

The density constitutes a crucial quantity for the dynamics of pedestrian flows (cf., e.g., as well Ref. [59]). While a value for the density can be enforced in simulations and to some extent in laboratory experiments as well, the value of the density in real-world pedestrian flows is often the consequence of the dynamics of the crowd, where individuals may even evaporate from the system, if not prevented by hard constraints which may result in crowd disasters. To use an analogy from equilibrium statistical mechanics, the density behaves like in a grand canonical ensemble where the chemical potential is given.

Within our particular setup the density plays a crucial role in the occurrence of the bifurcation scenario. At high densities the pedestrians jam in front of the obstacle, the dynamics changes considerably, pedestrians pass on each side of the obstacle, and the bistable dynamical behavior ceases to exist. Such phenomena occur if the interpersonal distance drops below 1 m, i.e., below the comfortable distance people prefer, or at an inflow rate to the channel which is higher than two individuals per second. We have tested these numbers extensively in simulations and in laboratory experiments with small groups of individuals. In fact, we have observed these problems when we run laboratory experiments without a controlled inflow since all participants may enter the corridor at the same time. In our laboratory setups we regulated the inflow to 0.6 persons/s.

At very low densities, in particular if the pedestrians do not notice each other any longer, no lemming effect dominates the motion, and the hysteresis disappears as well. Such features which also come with interruptions of the flow appear at interpersonal distances above 10 m. We have confirmed those values by extensive simulations of the setup used in our experiments and with preliminary experimental studies with small groups of people. In our laboratory experiments we have avoided these flow interruptions by a controlled inflow to the corridor.

The hysteresis occurs for a fairly broad range of densities with mean interpersonal distance between 1 and 10 m. While in simulations and laboratory experiments such a value can be achieved by controlling the inflow, most surprisingly the hysteresis also shows up in the field experiment where the inflow has not been monitored at all. Here the density itself fluctuates, and the interpersonal distance people prefer results in moderate densities which support the bistability. None of the aspects which come with real crowds of people such as fluctuation of the inflow, people deliberately ignoring the signs, families forming small groups within the stream of pedestrians, or asymmetries in the geometry of the corridor have resulted in a breakdown of the hysteresis phenomenon. In particular, unlike laboratory experiments, which are normally done by recruiting or even paying individuals, the people in our field experiment were not aware of what to expect, and that seems to be as well a crucial factor for the hysteresis phenomenon to occur. The bistability is therefore a representative scenario for people leaving or entering a domain freely, i.e., it is a characteristic feature for a crowd of pedestrians in an environment where they are able to ensure a comfortable distance between people, resulting in an effective average density which supports the occurrence of hysteresis.

Because of the discrete nature of counting people and given the moderate densities employed in our experiments, the signal processing had to cope with substantial finite-size effects, so that our setup cannot be captured by a continuum limit for the pedestrian flow. Such a challenge has an impact on the setup of the control loop, as the signal used to adjust the sign is initially discrete. Smoothing the signal by a simple low-pass filter turned out to be sufficient so that standard time continuous linear control theory could be applied.

Careful consideration is required to set up controlled experiments successfully. Artificial boundary conditions have the potential to destroy the dynamical features of realistic pedestrian flows. In that respect, any kind of periodic boundary conditions or repeated use of individuals have to be taken with a pinch of salt as the memory of individuals may induce novel dynamical properties which are otherwise absent. Hence the two types of experiments we have conducted were important: the laboratory-type experiment at the Ulmencampus (see Fig. 2) and the real-world application at the port of Warnemünde (see Fig. 3). In the former case, clear signage and instructions to the participants and a constant inflow avoiding disruption of the flow were crucial. Nevertheless, the qualitative dynamics of the flow is robust as proven by the comparison with the crowd in the Warnemünde port, where no particular instructions were given. However, in both cases it turned out to be necessary to prevent a disruption of the flow as otherwise the dynamical structures would have been erased from the system. Our Ulmencampus experiment succeeded as a test bed for emulating the behavior of real-world cohorts using a laboratory setup with fewer than 1000 participants. Within our setup we used a low-technology approach with regard to data recording and processing. Of course, more sophisticated data recording and data processing tools such as movement detection via video tracking could be used as well. However, our studies demonstrate that such advanced tools may not be required in general.

The approach we have used can be viewed as a particular installment of control-based continuation for complex systems, where one tracks unstable, unobservable states in relation to system parameters. Such features are crucial to understand the dynamical properties. Therefore our approach can be viewed as a particular variant of a spectroscopic tool. The unobservable dynamical features are the major lever for control with minimal impact, crowd management, and soft management strategies. In return, whenever a soft strategy is successfully applied, as, for instance, in dynamical speed limits [41,42], it is worth uncovering the underlying dynamical signature using a model-free approach. Furthermore, unstable states provide an important skeleton for any dynamical system, and any mathematical model has to reproduce such features. In that respect, our model-free and data-based approach can be used as well for benchmarking the accuracy of a dynamical model.

Crowd management is one of the key issues with huge impact on people's security and well-being as vividly illustrated by the recent need to implement effective social distancing measures to prevent diseases from spreading [9–11]. Understanding the dynamical aspects of large groups of pedestrians is at the heart of implementing control measures and designing related policies successfully. Our model-free approach can help to provide data and structures for soft management of people, e.g., understanding the effectiveness of signing systems and underpinning the results with dynamical features of the actual pedestrian flow. For instance, it is tempting to extend our approach to evacuation scenarios. While the lemming effect has a negative impact on the time needed to evacuate a room, it looks promising to use a combination of the existing knowledge based on mathematical models and a data-based model-free approach to find minimal invasive strategies for improving critical evacuation times of rooms and general infrastructure. We think our showcase may serve as a paradigm for future research in quantitative social science.

ACKNOWLEDGMENTS

The authors are greatly indebted to Ralf Ludwig from the Ulmencampus of the University of Rostock, to Oliver Schubert from F.C. Hansa Rostock, and to the Rostock Port authorities, in particular to Jens Käkenmeister and his colleagues, for supporting the experiments at their facilities. We are thankful to members of the Institute of Mathematics and other volunteers who helped us to conduct various experiments. J.S. thanks the DFG for support through the Collaborative Research Center CRC 1270 (Deutsche Forschungsgemeinschaft Grant No. SFB 1270/2–299150580). W.J. is grateful to EPSRC for financial support through Grant No. EP/R012008/1.

[1] S. P. Taylor, *The Hillsborough Stadium Disaster: 15 April 1989: Inquiry by the Rt Hon Lord Justice Taylor: Interim Report: Presented to Parliament by the Secretary of State for the Home Department by Command of Her Majesty August 1989* (HM Stationery Office, London, 1989).

[2] M. Pretorius, S. Gwynne, and E. R. Galea, Large crowd modelling: An analysis of the duisburg love parade disaster, Fire Mater. **39**, 301 (2015).

[3] K. Moodie, The King's Cross fire: Damage assessment and overview of the technical investigation, Fire Saf. J. **18**, 13 (1992).

[4] D. Helbing, A. Johansson, and H. Z. Al-Abideen, Dynamics of crowd disasters: An empirical study, Phys. Rev. E **75**, 046109 (2007).

[5] D. Helbing and A. Johansson, Pedestrian, crowd and evacuation dynamics, in *Encyclopedia of Complexity and Systems Science*, edited by R. Meyers (Springer, New York, NY, 2009).

[6] A. Schadschneider, W. Klingsch, H. Klüpfel, T. Kretz, C. Rogsch, and A. Seyfried, Evacuation dynamics: Empirical results, modeling and applications, in *Encyclopedia of Complexity and Systems Science* (Springer, New York, 2009), pp. 3142–3176.

[7] S. Sarkar, Qualitative evaluation of comfort needs in urban walkways in major activity centers, Transp. Q. **57**, 39 (2003).

[8] P. Dallard, T. Fitzpatrick, A. Flint, A. Low, R. R. Smith, M. Willford, and M. Roche, London Millennium Bridge: Pedestrian-induced lateral vibration, J. Bridge Eng. **6**, 412 (2001).

[9] P. Block, M. Hoffman, I. J. Raabe, J. B. Dowd, C. Rahal, R. Kashyap, and M. C. Mills, Social network-based distancing strategies to flatten the COVID-19 curve in a post-lockdown world, Nat. Hum. Behav. **4**, 588 (2020).

[10] E. Gibney, Whose coronavirus strategy worked best? Scientists hunt most effective policies, Nature (London) **581**, 15 (2020).

[11] N. Jones, How coronavirus lockdowns stopped flu in its tracks, Nature News, May 21, 2020.

[12] E. R. Galea, A general approach to validating evacuation models with an application to exodus, J. Fire Sci. **16**, 414 (1998).

[13] D. C. Duives, W. Daamen, and S. P. Hoogendoorn, State-of-the-art crowd motion simulation models, Transp. Res. Part C: Emerging Technol. **37**, 193 (2013).

[14] D. Chowdhury, L. Santen, and A. Schadschneider, Statistical physics of vehicular traffic and some related systems, Phys. Rep. **329**, 199 (2000).

[15] D. Helbing, I. Farkas, and T. Vicsek, Simulating dynamical features of escape panic, Nature (London) **407**, 487 (2000).

[16] D. R. Parisi, R. Cruz Hidalgo, and I. Zuriguel, Active particles with desired orientation flowing through a bottleneck, Sci. Rep. **8**, 9133 (2018).

[17] A. Kirchner, H. Klüpfel, K. Nishinari, A. Schadschneider, and M. Schreckenberg, Simulation of competitive egress behavior: comparison with aircraft evacuation data, Phys. A (Amsterdam) **324**, 689 (2003).

[18] M. Campanella, S. Hoogendoorn, and W. Daamen, Effects of heterogeneity on self-organized pedestrian flows, Transp. Res. Rec.: J. Transp. Res. Board **2124**, 148 (2009).

[19] *The Handbook of Tunnel Fire Safety*, edited by A. Beard and R. Carvel (Telford, London, 2005).

[20] M. Kobes, I. Helsloot, B. De Vries, and J. G. Post, Building safety and human behaviour in fire: A literature review, Fire Saf. J. **45**, 1 (2010).

[21] B. Steffen and A. Seyfried, Methods for measuring pedestrian density, flow, speed and direction with minimal scatter, Phys. A (Amsterdam) **389**, 1902 (2010).

[22] S. Heliövaara, J.-M. Kuusinen, T. Rinne, T. Korhonen, and H. Ehtamo, Pedestrian behavior and exit selection in evacuation of a corridor – An experimental study, Saf. Sci. **50**, 221 (2012).

[23] A. Nicolas, M. Kuperman, S. Ibañez, S. Bouzat, and C. Appert-Rolland, Mechanical response of dense pedestrian crowds to the crossing of intruders, Sci. Rep. **9**, 105 (2019).

[24] A. Garcimartín, J. Pastor, C. Martín-Gómez, D. Parisi, and I. Zuriguel, Pedestrian collective motion in competitive room evacuation, Sci. Rep. **7**, 10792 (2017).

[25] D. Helbing, L. Buzna, A. Johansson, and T. Werner, Self-organized pedestrian crowd dynamics: Experiments, simulations, and design solutions, Transp. Sci. **39**, 1 (2005).

[26] M. Boltes and A. Seyfried, Collecting pedestrian trajectories, Neurocomputing **100**, 127 (2013).

[27] A. Corbetta, L. Bruno, A. Muntean, and F. Toschi, High statistics measurements of pedestrian dynamics, Transp. Res. Proc. **2**, 96 (2014).

[28] A. Banerjee, A. K. Maurya, and G. Lämmel, A review of pedestrian flow characteristics and level of service over different pedestrian facilities, Coll. Dyn. **3**, A17 (2018).

[29] L. D. Vanumu, K. R. Rao, and G. Tiwari, Fundamental diagrams of pedestrian flow characteristics: A review, Eur. Transp. Res. Rev. **9**, 49 (2017).

[30] S. P. Hoogendoorn and W. Daamen, Pedestrian behavior at bottlenecks, Transp. Sci. **39**, 147 (2005).

[31] A. Jelic, C. Appert-Rolland, S. Lemercier, and J. Pettre, Properties of pedestrians walking in line: Fundamental diagrams, Phys. Rev. E **85**, 036111 (2012).

[32] J. Zhang and A. Seyfried, Empirical characteristics of different types of pedestrian streams, Proc. Eng. **62**, 655 (2013).

[33] M. Moussaid, E. G. Guillot, M. Moreau, J. Fehrenbach, O. Chabiron, S. Lemercier, J. Pettré, C. Appert-Rolland, P. Degond, and G. Theraulaz, Traffic instabilities in self-organized pedestrian crowds, PLoS Comput. Biol. **8**, e1002442 (2012).

[34] A. Corbetta, J. A. Meeusen, C. Lee, R. Benzi, and F. Toschi, Physics-based modeling and data representation of pairwise interactions among pedestrians, Phys. Rev. E **98**, 062310 (2018).

[35] A. Schadschneider and A. Seyfried, Empirical results for pedestrian dynamics and their implications for modeling, Networks Heterog. Media **6**, 545 (2011).

[36] P. Geoerg, J. Schumann, M. Boltes, and M. Kinateder, How people with disabilities influence crowd dynamics of pedestrian movement through bottlenecks, Sci. Rep. **12**, 14273 (2022).

[37] C. Harrison, N. Kukadia, P. Stoneman, and G. Dyer, *Pilot for standing on both sides of escalators, in Proceedings of the 6th Symposium on Lift and Escalator Technologies* (University of Northampton, Northampton, 2016), pp. 11-1–11-10.

[38] R. Challenger, C. W. Clegg, and M. A. Robinson, Understanding Crowd Behaviours: Guidance and Lessons Identified (Cabinet Office Emergency Planning College, Easingwold, UK, 2009).

[39] S. A. Richmond, A. R. Willan, L. Rothman, A. Camden, R. Buliung, C. Macarthur, and A. Howard, The impact of pedestrian countdown signals on pedestrian-motor vehicle collisions: a reanalysis of data from a quasi-experimental study, Inj. Prev. **20**, 155 (2014).

[40] See Supplemental Material at http://link.aps.org/supplemental/10.1103/PhysRevResearch.4.043190 for a blurred video sequence of the transition in route choice of the pedestrian flow experiment at the Ulmencampus of the University of Rostock (2022).

[41] R. L. Bertini, S. Boice, and K. Bogenberger, Dynamics of variable speed limit system surrounding bottleneck on German Autobahn, Transp. Res. Rec.: J. Transp. Res. Board **1978**, 149 (2006).

[42] B. Khondaker and L. Kattan, Variable speed limit: A microscopic analysis in a connected vehicle environment, Transp. Res. Part C: Emerging Technol. **58**, 146 (2015).

[43] C. Fuhs and P. Brinckerhoff, *Synthesis of Active Traffic Management Experiences in Europe and the United States*, Tech. Rep. FHWA-HOP-10-031 (U.S. Federal Highway Administration, Washington, DC, 2010).

[44] T. Shinbrot, C. Grebogi, J. A. Yorke, and E. Ott, Using small perturbations to control chaos, Nature (London) **363**, 411 (1993).

[45] C. I. Siettos, I. G. Kevrekidis, and D. Maroudas, Coarse bifurcation diagrams via microscopic simulators: A state-feedback control-based approach, Int. J. Bifurcation Chaos **14**, 207 (2004).

[46] S. Misra, H. Dankowicz, and M. R. Paul, Event-driven feedback tracking and control of tapping-mode atomic force microscopy, Proc. R. Soc. A **464**, 2113 (2008).

[47] J. Sieber and B. Krauskopf, Control based bifurcation analysis for experiments, Nonlinear Dyn. **51**, 365 (2008).

[48] D. A. Barton and J. Sieber, Systematic experimental exploration of bifurcations with noninvasive control, Phys. Rev. E **87**, 052916 (2013).

[49] J. Sieber, A. Gonzalez-Buelga, S. Neild, D. Wagg, and B. Krauskopf, Experimental Continuation of Periodic Orbits through a Fold, Phys. Rev. Lett. **100**, 244101 (2008).

[50] E. Bureau, F. Schilder, I. F. Santos, J. J. Thomsen, and J. Starke, Experimental bifurcation analysis of an impact oscillator–tuning a non-invasive control scheme, J. Sound Vib. **332**, 5883 (2013).

[51] K. Pyragas, V. Pyragas, I. Kiss, and J. Hudson, Stabilizing and Tracking Unknown Steady States of Dynamical Systems, Phys. Rev. Lett. **89**, 244103 (2002).

[52] C. W. Gear, J. M. Hyman, P. G. Kevrekidis, I. G. Kevrekidis, O. Runborg, and C. Theodoropoulos, Equation-free, coarse-grained multiscale computation: Enabling microscopic simulators to perform system-level analysis, Commun. Math. Sci. **1**, 715 (2003).

[53] N. Bellomo and C. Dogbe, On the modeling of traffic and crowds: A survey of models, speculations, and perspectives, SIAM Rev. **53**, 409 (2011).

[54] E. Papadimitriou, G. Yannis, and J. Golias, A critical assessment of pedestrian behaviour models, Transp. Res. Part F: Traffic Psychol. Behav. **12**, 242 (2009).

[55] A. L. Bazzan and F. Klügl, *Multi-agent Systems for Traffic and Transportation Engineering* (Information Science Reference, Hershey, PA, 2009).

[56] D. Helbing and P. Molnar, Social force model for pedestrian dynamics, Phys. Rev. E **51**, 4282 (1995).

[57] J. Starke, K. B. Thomsen, A. Sørensen, C. Marschler, F. Schilder, A. Dederichs, and P. Hjorth, Nonlinear effects in examples of crowd evacuation scenarios, in *17th International IEEE Conference on Intelligent Transportation Systems (ITSC)* (IEEE, Qingdao, China, 2014), pp. 560–565.

[58] I. Panagiotopoulos, J. Starke, J. Sieber, and W. Just, Continuation with non-invasive control schemes: Revealing unstable states in a pedestrian evacuation scenario, arXiv:2203.02484 [math.DS] [SIAM J. Appl. Dyn. Syst. (to be published)].

[59] I. Echeverría-Huarte, A. Garcimartín, R. C. Hidalgo, C. Martín-Gómez, and I. Zuriguel, Estimating density limits for walking pedestrians keeping a safe interpersonal distancing, Sci. Rep. **11**, 1534 (2021).